DETECTION OF PAD CRATER INITIATION IN SHOCK USING ACOUSTIC EMISSION DETECTION

W. Carter Ralph
Southern Research Institute
Birmingham, AL, USA
ralph@southernresearch.org

Gregory N. Morscher
The University of Akron
Akron, OH, USA

Elizabeth Elias Benedetto
Hewlett-Packard
Houston, TX, USA

Keith Newman and Aileen Allen
Hewlett-Packard
Palo Alto, CA, USA

Julie Silk
Keysight Technologies
Santa Rosa, CA, USA

ABSTRACT
Acoustic emission detection was used to identify damage events on electronic assemblies during mechanical shock testing. Two board designs manufactured from several laminate types were instrumented with acoustic transducers and dropped multiple times at acceleration levels between 100 and 250*g*. Acoustic events that indicated a failure within the footprint of the ball grid array were identified and located using triangulation. Dye stain and cross section failure analysis techniques were used to identify pad crater damage and showed good agreement with the acoustic events. The results indicate that acoustic emission detection can be used to identify and locate pad cratering during shock within approximately 5 mm, and has the potential to significantly improve the speed and precision of mechanical shock testing.

INTRODUCTION
Detection of interconnect damage initiation has been a challenge for the electronics industry. Current mechanical shock test methods typically use a combination of strain gage measurements, electrical continuity monitoring, and destructive post-test failure analysis. These processes can be imprecise and time-consuming, and are often not feasible on fully-populated production assemblies. Acoustic emission detection is a potential technique for identifying the stress level and location of interconnect fractures during mechanical shock tests, which could improve the quality of the test while decreasing the required cost and time.

Acoustic emission techniques have been in development and use since the 1950s. Active acoustic emission is used to detect sub-surface flaws, while passive acoustic emission detection (AED) is used to detect fracture events during structural loading. The passive AED technique typically employs an array of transducers to measure surface sound waves; the location of the fracture event is calculated using the positions of the sensors, the time delay between the arrival of the events at the sensors, and the sonic velocity through the medium.

The use of AED for the electronics industry was first published in 2011, in which two acoustic sensors were used to detect fracture events in a four point bend test [1]. This allowed events to be located in one dimension and matched with the time, strain, and displacement measurements. Subsequent studies used four sensors to detect fractures in four point bend [2] and in the industry-standard spherical bend test [3,4,5] to locate the events in two dimensions across the board surface. These later studies correlated the relative intensity of the acoustic events with pad crater events in order to differentiate between interconnect damage and other non-critical acoustic events. This demonstrated the identification of the precise moment of interconnect damage, the location of the damage to regions of the ball grid array, and that the precision and speed of the test method could be greatly improved through the use of AED.

This work led to the question of whether AED could be applied to mechanical shock testing. There are several challenges to using AED in shock. Transient bend testing is relatively slow (about 500 milliseconds from initial loading to the initiation of interconnect damage) compared to shock testing. This means that the acoustic events happen much closer together in time, with the events and the reflections of the acoustic waves potentially overlapping each other. Due to the highly dynamic nature of the test, shock induces much more noise from the fixtures and the instrumentation, which could be mistaken for interconnect damage.

Previous work examined initial investigations into the feasibility of assessing shock using AED on a single test board design [6]. This paper presents two rounds of shock tests from 100 to 200*g* that employed AED to detect interconnect damage events. Both multiple and single drops were performed, and two different board designs were tested. Failure analysis was performed on the post-test boards to determine the extent and location of pad craters, if any. The acoustic data were analyzed to identify the presence and location of acoustic events that were indicative of fractures. The acoustic and failure analysis data were compared.

TEST AND DATA REDUCTION METHODS

Two test board designs were evaluated: a 35x35 mm PBGA package on a 1.6 mm thick 203x203 mm board and a 45x45 mm SBGA on a 1.6 mm thick 173x104mm board, both of which are shown in Figure 1. The PBGA packages were mounted using metal defined pads with 1 mm pitch SAC305 solder, and the boards were made from two different 0/90 layup laminate materials. The SBGA packages were mounted using metal defined pads with 1.27 mm pitch SAC305 solder, and the boards were constructed using three different laminates.

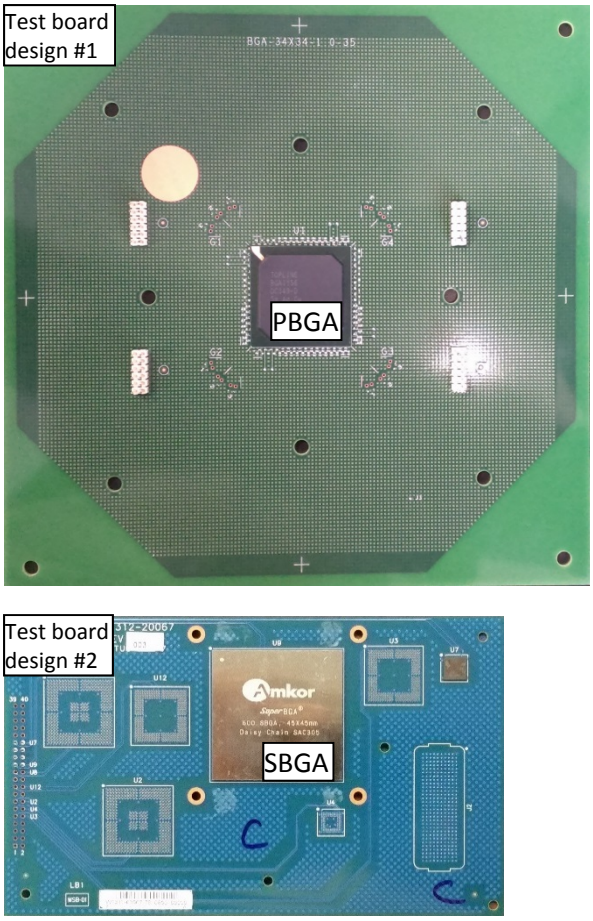

Figure 1. Test Boards

The shock tests were performed at a variety of acceleration levels with 2 ms half-sine input pulses. Since there was neither a specific end product configuration nor a specific use condition, these parameters were selected to be generally representative of typical test conditions and to straddle the threshold for damage. These conditions also align with the range of conditions included in JEDEC JESD22-B110B. The goal was to perform tests that either induced no damage or partial damage so that the acoustic emission analysis could provide meaningful positive and negative failure assessments. The pulse duration and half-sine pulse shape were controlled by felt damping pads and were calibrated before each new input acceleration level. The shock setup is shown in Figure 2. The boards were mounted with the package facing down so that the interconnections were loaded in tension first. A multi-axis accelerometer was mounted on the shock table to measure the input conditions. The acoustic transducers were mounted at the corners of each package using a thin layer of accelerometer wax. In order to keep the instrumentation wires from slapping the board during impact, wires were taped to the board with masking tape and the point of contact with the board was secured with putty.

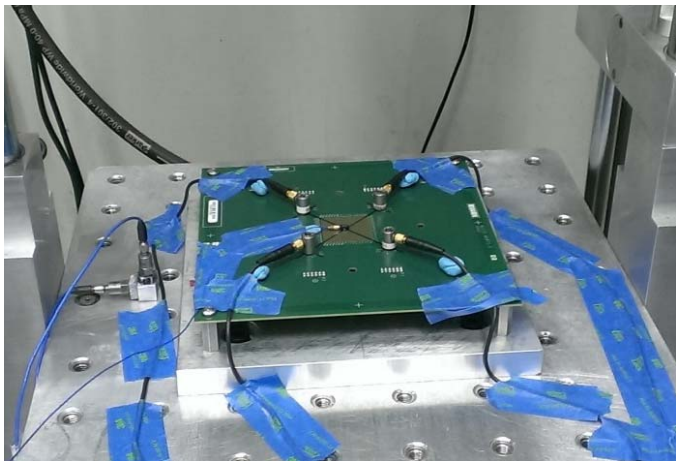

Figure 2. Shock Test Setup

In order to determine the mechanical shock level at which pad craters would occur, several boards were subjected to a single shock test without acoustic instrumentation. These boards were evaluated using layout dye stain testing and the results were used to determine the range of acceleration levels for the subsequent shock tests with acoustic data acquisition. The results from these preliminary tests are shown in Table 1. From these results, it was determined that 100*g* was an appropriate negative test level (no expected interconnect failures), and that 150-250*g* would be the range likely to produce positive tests for the PBGA boards. The minimum test apparatus level of 100*g* would be used to attempt to produce negative tests for the SBGA boards, while higher levels would be likely to produce positive tests.

Table 1. Preliminary Shock Test Results

Board Type	**Shock Level (*g*)**	**Number of Drops**	**Dye Stain Results**
PBGA	100	1	No opens
PBGA	150	1	No opens
PBGA	250	1	2 partial cracks
PBGA	350	1	Partial and full cracks across component
PBGA	450	1	Full opens across most of component
SBGA	125	1	Very small partial cracks in three corners
SBGA	150	1	Partial cracks in all four corners
SBGA	175	1	Partial and full opens in all four corners

Acoustic data were recorded with a modal acoustic emission system using an array of four acoustic emission transducers, which are approximately 9mm in diameter. This system continuously records data to buffer, and saves a pre-set amount of waveform data whenever the signal exceeds a threshold. The sampling rate was 5 MHz, and either 16384 or 8192 acoustic waveform data points were saved post-trigger, while 1638 points were saved pre-trigger. A 50 kHz high pass hardware filter was set on the signal, and a 1.5 MHz low pass filter was set on the trigger. The overall pre-amp was typically set at 24 dB; the recorded signal was amplified 18 dB; and the trigger was amplified 6 dB. Additional acoustic data were recorded with a digital oscilloscope using an array of four 8 mm diameter acoustic emission transducers. The transducer array was positioned with a sensor just outside of each corner of the package on the back (non-package) side of the board, as shown in Figure 2.

Acoustic data was analyzed post-test by first assessing events which were known to have occurred within the sensor array. Figure 3 illustrates two typical waveform types that were analyzed, showing screen captures: (a) a set of waveforms captured on all four sensors on panel Z992 during the impact phase of a 225*g* shock test; (b) a set of waveforms capturing a subsequent transient event during the 225*g* shock test, which were associated with fracture events in the board. For the AE capture settings used, typical waveform capture windows lasted for either 819 or 1638 microseconds and would frequently include several distinct acoustic events, as in Figure 3b, where there is a smaller amplitude event at the beginning of the capture window and a higher amplitude event towards the end of the window. Only events in which there was confidence that the event had occurred within the sensor array were analyzed. The criteria for events of interest were as follows: (1) pulses within a given waveform that were clearly recorded on each sensor; (2) pulses with a clear first peak which pertained to the extensional part of the waveform on at least the three sensors closest to the source; (3) pulses that had a high amplitude (> 0.7 V) for the pulse with the earliest time of arrival. The clear first peak was necessary in order to estimate the location and it was assumed that higher amplitude events that clearly emanated from within the sensor array were from a damage event within the board or package.

The locations of events were then determined by triangulation from the times of arrival for the pulses using equations 1, 2, and 3, where x and y are the coordinates in an x-y grid, the subscript pertains to the locations of the transducers, C_c is the speed of sound in this material (3200 m/s) and t is the arrival time at a given sensor. Boron fiber breaks were used to create acoustic source events of a known location to measure the speed of sound in the material and to determine the accuracy of the triangulation method. Figure 4 shows sensor location (large circles) and lead-break location (small filled circles) for an undamaged board. The open circles estimate the boron fiber break location from triangulation equations. It was found that, in all but one case, the accuracy of the triangulation method was within +/- 5 mm of the sensor location.

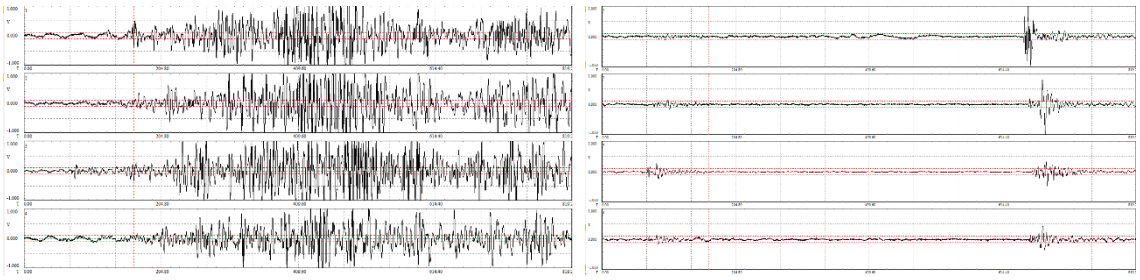

(a) (b)

Figure 3. Typical Waveforms in the Shock Tests Indicating (a) the shock event and (b) potential damage events

$$\sqrt{(x-x_3)^2+(y-y_3)^2}-\sqrt{(x-x_2)^2+(y-y_2)^2}=C_c(t_3-t_2) \quad \text{(Eqn. 1)}$$

$$\sqrt{(x-x_4)^2+(y-y_4)^2}-\sqrt{(x-x_2)^2+(y-y_2)^2}=C_c(t_4-t_2) \quad \text{(Eqn. 2)}$$

$$\sqrt{(x-x_1)^2+(y-y_1)^2}-\sqrt{(x-x_2)^2+(y-y_2)^2}=C_c(t_1-t_2) \quad \text{(Eqn. 3)}$$

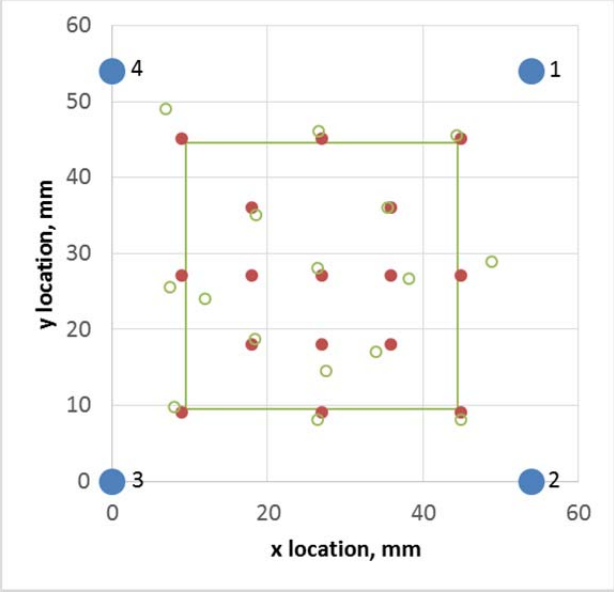

Figure 4. Sensor Location and Lead-Break Location for an Undamaged Board

RESULTS

The AE data were examined from selected boards that were subjected to shock tests. In some cases multiple shock tests were performed on a single board. Either dye staining or cross-sectional analyses were used on a subset of boards after the acoustic emission testing to validate whether acoustic events of interest were the result of pad cratering events. Results from boards with failure analysis data are listed in Table 2.

There were several considerations and complications in analyzing the acoustic data: the nature of shock tests, the difficulty in separating out signals of interest, and the inability to acquire all the pertinent acoustic data due to equipment limitations (acquisition blackout times).The shock test consists of a number of mechanical events that can generate acoustic events. The shock table first contacts the base plate of the shock equipment, the table then decelerates to a stop, followed by a rebounding of the board at its natural frequency. Interconnect damage is most likely to occur as the table comes to a stop and the interconnections are loaded in tension. Damage may also occur at each subsequent rebound.

There is considerable acoustic activity generated by the impact event, damage in the board material, reflections of acoustic waves from board features (such as edges and holes), instrumentation wires, and the impingement of the board on the support pins. The damage to the interconnections are the events of interest. Sorting out the pertinent data requires good correlation between the appropriate signals and quantifiable damage.

The computer acquires data within a fixed time window, for this investigation either 1638 microseconds (8192 points at 5 MHz capture rate) or 819 microseconds (4096 points at 5 MHz capture rate). The computer then needs to rearm in order to save the next waveform. In the first round of testing it appeared that a significant amount of data was lost just after impact due to the re-arming of the AE system. A second set of tests was conducted using an order of magnitude longer capture window to mitigate this situation.

The failure analysis performed on these boards consisted of dye stain for the majority of the boards and cross-sectional analysis for Z796, D160, and E175. The concern with layout dye staining was that if the laminate cracks were initiating within the board material without opening to the surface, failures would not be observed with this method. For example, the AE data indicated a possible crack on one corner of 1A027, which was not found with dye staining. Unfortunately, it is not possible to go back to a board that

has been though the dye stain process and check for laminate cracking via other means, as the component removal process may induce damage that would be incorrectly assessed as laminate cracking. Therefore, cross-sectioning was chosen for a set of the test boards in this study. Dye staining does, however, show correlation when the cracks are large enough to reach the external layers of board, as we see in the correlation between the AE data and the dye stain results for board 1A030 (Figure 5)

Table 2. Shock Tests, AE Results and Failure Analysis Results

Board	Drop Inputs	FA Results	Acoustic Events
Z986	1 @ 250*g*	Dye stain: 3 partials at corner 1	High amplitude event near corner 1
Z988	8 @ 130*g*	Dye stain: no opens found	Several high amplitude events around corner 2
Z990	1 @ 175*g*	Dye stain: sensor 3 one partial	Only one high amplitude event on near 2 and lower amplitude events near 3
Z991	5 @ 150*g*	Dye stain: no opens found	One high amplitude event at 3
Z992	5 @ 150 to 225*g*	Dye stain: 1 partial sensor 1 and 2 partials sensor 3	Multiple high amplitude events near sensors 1 and 3 and a single event near sensor 2
Z997	10 @ 100*g*	Dye stain: no opens found	No high amplitude events
1A027	1 @ 200*g*	Dye stain: no opens found	High amplitude event near corners 1 and 2, medium event near 1
1A030	1 @ 200*g*	Dye stain: partial open at corner 3	Medium amplitude events near corners 2 and 3
Z976	1 @ 225*g*	Cross section: partial cracks at corners 1 and 3, die cracking	Several high amplitude events at 1 and two moderate events at 4
D160	2 @ 175*g*	Cross section: partial cracks at all corners, with multiple partials at 3	One medium amplitude event near 4 and one near 3
E175	1 @ 125*g*	Cross section: partial crack at corner 3	One medium amplitude event near 3 and one near 1

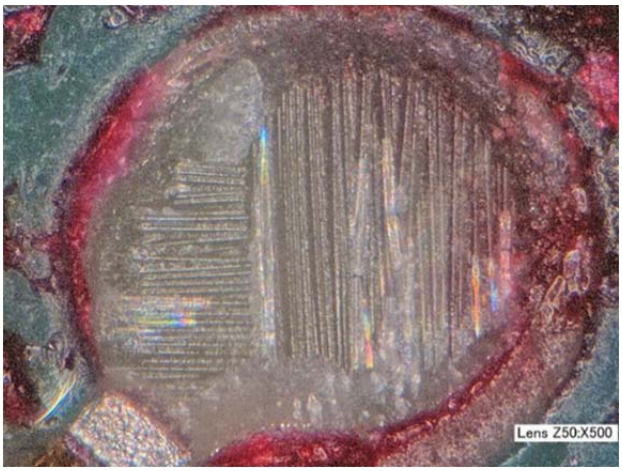

Figure 5. Dye Stain Partial Crack Seen on Board 1A030 Corner 3

An interesting acoustic signal seen in board 0Z976 indicated an event occurring at the center of the board, which was not expected as the pad cratering typically occurs in the corner locations. Cross-sectional analysis of this board identified several laminate cracks under corner locations, but also identified evidence of die cracking which is likely the source of the acoustic signal located at the center of the package. Images of both the laminate and die cracks can be seen in Figures 6 and 7.

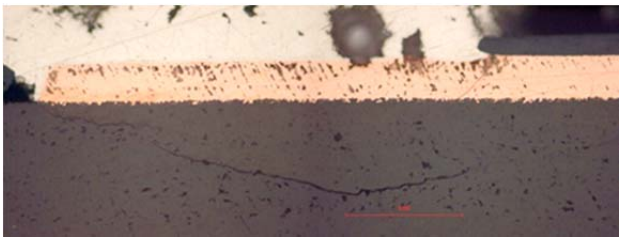

Figure 6. Laminate Cracks Seen on Board 0Z976 Corner 3

Figure 7. Die Cracking on Board 0Z976

As this investigation progressed, it was evident that we were seeing better correlation with cross-sectional analysis than with dye stain. Figures 8 and 9 show cross-sections of the final two boards tested in this study. As stated previously, this is more likely a limitation of the dye stain test process than with the acoustic emission methodology. Cross-sectioning, while more time consuming, is able to identify smaller cracks within the laminate that may not be detected using dye stain. The limitation of cross-sectioning is that a good deal of the sample is destroyed in order to grind to the location of interest and, in some cases, one location of interest must be sacrificed in order to inspect another

location of interest. Although there were some component corners which were not investigated, the ones where we expected to see a crack due to the AE signal, did indeed result in a crack seen in the cross-sectional analysis. This suggests that AE is a more sensitive method in identifying pad craters than dye stain, and possibly more useful than cross-sectioning, if we take the difficulty of inspecting all possible crack locations into account.

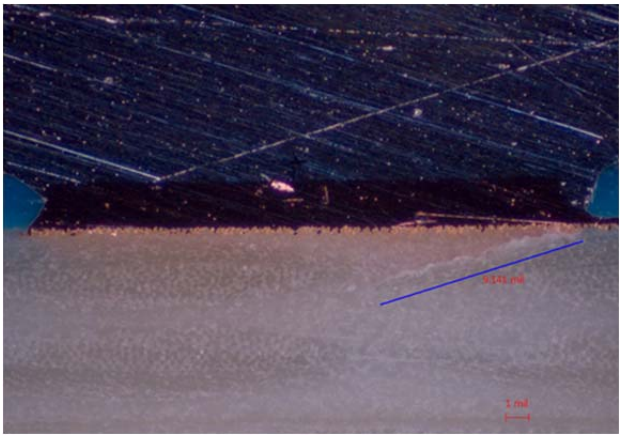

Figure 8. Board E175, Partial Crack Under Corner 3

Figure 9. Board D160 Multiple Partial Cracks Under Corner 3

Two of the most successful correlations with the dye stain results were for boards Z986 and Z992. Figure 10 shows acoustic regions of interest from the pertinent waveforms for (a) board Z986 after 275*g* shock and (b) board Z992 after 225*g* shock. The frequency content of these waveforms is primarily in the 100 to 300 kHz range. The first peaks from which location analysis was performed are identified with arrows. Note that the Z986 test had the lower preamp setting but had the higher energy pulse (several peaks > 1 V). This was the only event in this test that showed a very high signal intensity of all the events which occurred within the sensor array. All other events appeared more like the event in Figure 10(b), where only one or two peaks of a given pulse exhibited a high amplitude.

The location analysis for the two tests is shown in Figure 11. Board Z986 showed significant damage around sensor 1, which was in the region where the high energy event occurred within 0.016 microseconds of the initial acoustic signal associated with the shock event. The Z992 board drops exhibited events which occurred primarily on sensors 1 and 3 in the sequential shock tests with increasing acceleration. Note that one event did occur near sensor 2 but the other seven events occurred near sensors 1 and 3, which corresponded with dye staining.

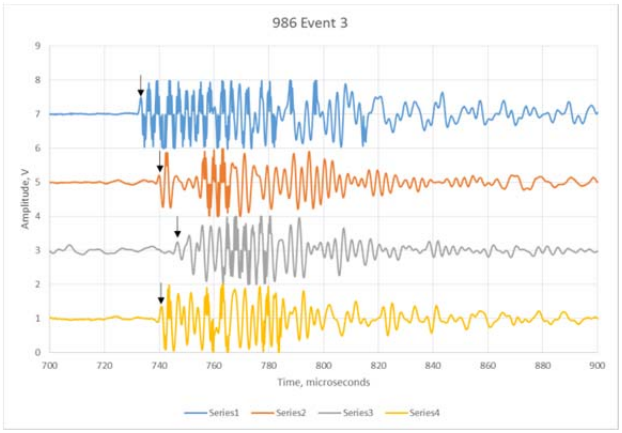

(a)

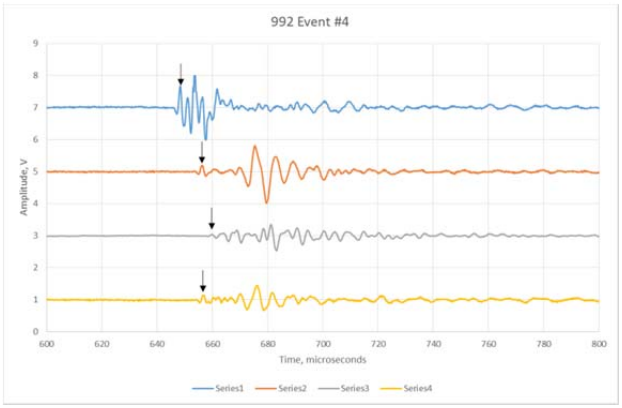

(b)

Figure 10. (a) The High Energy Event from Z986 after 275g Shock and (b) the Pulse Later in the Waveform

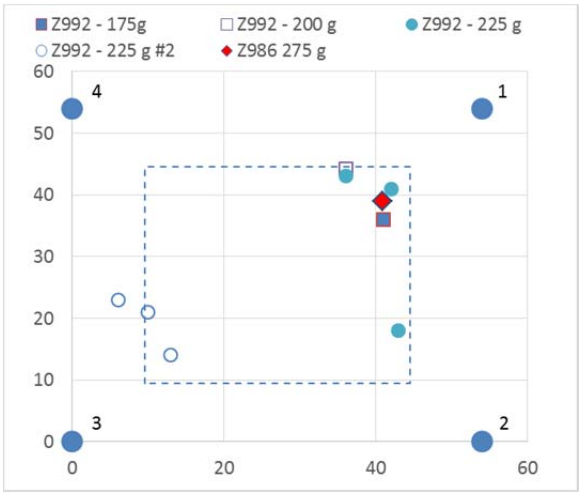

Figure 11. Location Analysis of Pulse Events from the Two Different Shock Tests for Panels Z986 and Z992

A high-speed camera (16 mm lens, 5000 frames per second, 6.7µs shutter opening, 5x100W LED lighting) was used to monitor selected drop tests. The camera was mounted slightly below the plane of the test board (Figure 12). The board edge was marked at ½ inch intervals with black marker to provide distance calibration and tracking targets. The acquired high speed video was post-processed using video analysis software.

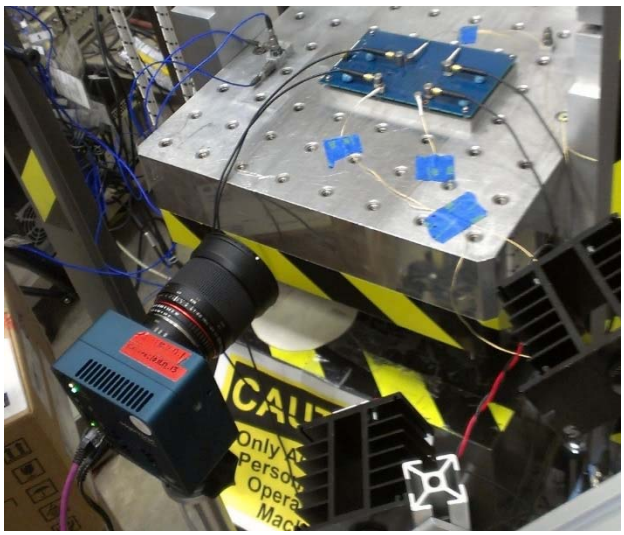

Figure 12. High-Speed Camera

Three tests were successfully recorded. In each case the video clearly shows the moment of impact and the subsequent flexing of the board. The boards took between 1.4 and 2.8 milliseconds to reach their maximum flexure after impact, and then rebounded at their natural frequencies.

In one of the videos (board KP160) AE Transducer 3 was dislodged and struck both the board and the adjacent oscilloscope transducer several times, providing distinct time markers in the acoustic data. These markers were used to synchronize the acoustic emission and oscilloscope data with the video.

Figure 13 shows the AE waveform data from all four AE sensors (designated "AE#") pieced together from several events that were triggered and captured. Note that blank space in between data is due to the AE system not being triggered. Also shown is the data captured from the oscilloscope on sensors 1 and 3 to compare the farthest oscilloscope sensor from AE sensor impact with the nearest oscilloscope sensor to AE sensor impacts. Also shown are three frame captures from the video which could clearly be correlated with oscilloscope and/or AE waveform features.

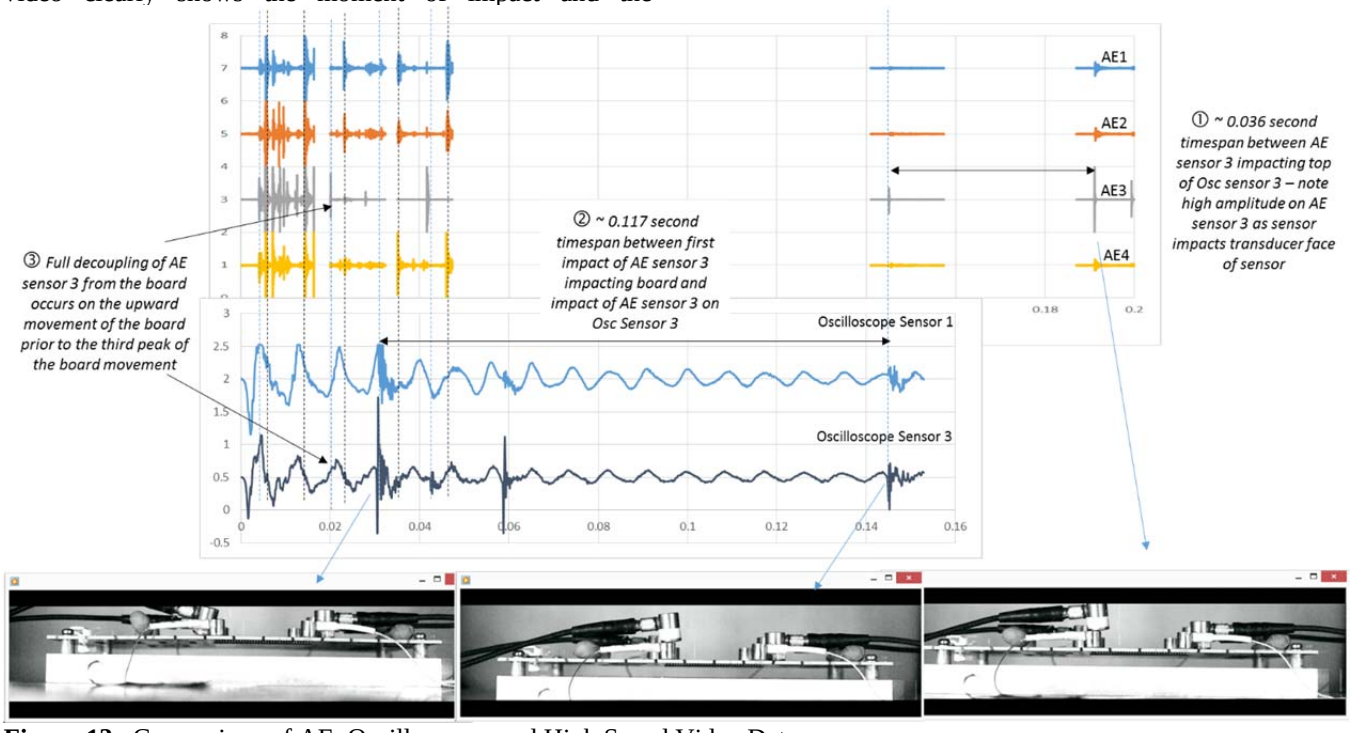

Figure 13. Comparison of AE, Oscilloscope, and High Speed Video Data

Caption 1 corresponds to the events which occurred later in the test and have the clearest correlation between AE and oscilloscope since damage events are not occurring at the same time. The AE sensor struck the oscilloscope sensor at times of approximately 0.145 and 0.191 seconds. From this the AE and oscilloscope data could be clearly synchronized based on the event that corresponds to 0.145 seconds (the oscilloscope stopped recording data after 0.15 seconds). Note that for these two sensor-to-sensor impact events, the AE sensor struck the oscilloscope sensor flat on its face so that there was a very large amplitude peak on AE sensor 3, but much lower amplitude on the other AE sensors since the event had to travel through the oscilloscope sensor and the board to those sensors.

Caption 2 corresponds to the timespan between the very first AE sensor-to-board impact event and the clearly identified 0.145 sec impact event. The timing between AE, oscilloscope and video all match in time for these two impact events enabling full correspondence between the three data captures. Note that for the first impact event, very little amplitude is recorded on AE sensor 3, whereas there are events captured shortly afterwards on the other AE sensors. The corresponding video image shows that the AE sensor struck the board on its edge rather than its face, which would not transmit much amplitude to the sensor.

Caption 3 corresponds to the initial full decoupling of AE sensor 3 from the board, which occurred on the upward movement of the board just prior to the third peak. This is in good correspondence with the oscilloscope Sensor 3 movement and the time between the two oscilloscope events indicated by the arrows.

Finally, it was evident that the (unfiltered) oscilloscope output was in sync with the up and down oscillation of the board based on the two events described above. In other words, even though the sensor is tuned to higher frequency range than the board movement, it still captured the peaks and valleys of the board oscillation. In addition, the absolute time that an event is recorded on the AE system is only accurate to the millisecond decimal; therefore, the AE sensor time is +/- 0.0005 seconds from that shown in Figure 10. Nevertheless, it is apparent that groups of acoustic activity picked up on the AE system correspond to the periods of upward and downward movement of the board. However, the timing of those groups appear to be nearer to the zero position of the board amplitude (black lines in Figure 13) rather than the peak or valley.

CONCLUSIONS

These results demonstrate that acoustic emissions from interconnect fractures can be detected in mechanical shock. The failures that were recorded corresponded to pad craters, which is a common failure mode. The locations of the pad crater events can be located within approximately 5 mm. This initial study demonstrated that AE can detect small amounts of pad cratering during mechanical shock, often at the early crack-initiation phase. Physical failure analysis using cross-sectioning produced no observed false positives or negatives. Dye-stain could not confirm all failures detected with AE, likely due to lack of crack penetration to the surface. Further refinement in test equipment, pre-amplification settings and filtering are needed to ensure complete event capture, and reduction in the number of observed false-failures.

Acoustic emission is a promising method for detecting damage in mechanical shock. It has the potential to detect damage relatively quickly, cheaply, and accurately. Further use and development by the electronics industry is warranted.

ACKNOWLEDGMENTS

As is often the case, this study was made possible only by wide-ranging contributions from a number of individuals. The authors would particularly like to express their thanks to David Moore (HP, high-speed camera), Dr. Punan Tang and Floyd Privette (HP, mechanical shock), John Vijil (HP, AE), Ron Salinas (HP, failure analysis), and Mr. Joshua Vijayam (Southern Research).

REFERENCES

1. Bansal, A New Approach for Early Detection of PCB Pad Cratering Failures, IPC APEX EXPO Proceedings, Las Vegas, NV, 2011.
2. Bansal, Guirguis, and Liu, Investigation of Pad Cratering in Large Flip-Chip BGA using Acoustic Emission, IPC APEX EXPO Proceedings, San Diego, CA, 2012.
3. Ralph, Daspit, Cain, Benedetto, Jenkins, Allen, and Newman, Acoustic Emission Detection of BGA Components in Spherical Bend, Proceedings of the Electronic Components and Technology Conference, Las Vegas, NV, pages 208-213, 2013.
4. Ralph, Daspit, Cain, Benedetto, Jenkins, Allen, and Newman, Acoustic Waveform Energy as an Interconnect Damage Indicator, Conference Proceedings of the Society for Experimental Mechanics, pages 33-42, 2014.
5. Ralph, Benedetto, Allen, and Newman, Pad Crater Detection Using Acoustic Waveform Analysis, Proceedings of the Electronic Components and Technology Conference, Orlando, FL, pages 1433-1440, 2014.
6. Ralph, Benedetto, Morscher, Newman, and Silk, Detecting Interconnect Damage in Shock Using Acoustic Emission Detection, Conference Proceedings of the Society of Experimental Mechanics, 2015.